Analysis of Transient Electromagnetic Scattering from an Overfilled Cavity Embedded in an Impedance Ground Plane

Robert S. Callihan and Aihua W. Wood

Department of Mathematics and Statistics
Air Force Institute of Technology, Wright-Patterson AFB, Ohio 45433-7765, USA
robert.callihan@us.af.mil, aihua.wood@afit.edu

Abstract **—** In this paper, we consider the time-domain scattering problem of a two-dimensional overfilled cavity embedded in an impedance ground plane. An artificial boundary condition is introduced on a semicircle enclosing the cavity that couples the fields from the infinite exterior domain to those fields inside. The problem is first discretized in time using the Newmark scheme, and at each time step, we derive the variational formulation for the TM polarization, and establish well-posedness. Numerical implementation of the method for both the planar and overfilled cavity models is also presented.

Index Terms **—** Impedance boundary conditions, overfilled cavity, time domain.

I. INTRODUCTION

Electromagnetic scattering of cavity-backed apertures has been examined by numerous researchers in the engineering community (for example [1-6]) and the mathematical community (for example [7-10]). For overfilled cavities, we mention the works [11-14]. We note that most of the published work deals with either cavities with PEC ground planes or time-harmonic problems. Here, we consider transient overfilled cavities with impedance boundary conditions. Our approach is unique in that we develop a hybrid finite element - boundary integral mathematical model that incorporates an overfilled cavity with impedance boundary conditions. It will be more mathematically challenging yet more physically realistic and, as a result, has numerous applications.

We organize the paper as follows. In Section II, we introduce the problem setting and geometry. In Section III, we discretize the PDE via the Newmark scheme, first decomposing the entire solution domain into two sub-domains via an artificial semicircle, $\mathcal{B}_R$, which entirely encloses the overfilled cavity. This requires solving a nonhomogeneous modified Helmholtz equation with nonhomogeneous impedance boundary conditions at each time step via a generalized Green's function approach to obtain an integral representation. In Section IV, we present the integral representation, the Green's function for an impedance ground plane, and the properties of the Steklov-Poincaré operator. We conclude in Section V, by producing a variational formulation of the problem that is well-posed. In Section VI, we provide numerical results for a simplified planar cavity and an overfilled cavity that demonstrates the analysis can be implemented.

II. PROBLEM SETTING

Let $\Omega \subset \mathbb{R}^2$ be the cross-section (cavity interior) of a z-invariant cavity in the infinite ground plane, and the infinite homogenous, isotropic region above the cavity as $\mathcal{U} = \mathbb{R}^2_+ \setminus \Omega.$ Furthermore, let $\mathcal{B}_R$ be a semicircle of radius R, centered at the origin and surrounded by free space, large enough to completely enclose the overfilled portion of the cavity. We denote the region bounded by $\mathcal{B}_R$ and the cavity wall S as Ω_R, so that Ω_R consists of the cavity itself and the homogeneous part between $\mathcal{B}_R$ and Γ. Let $\mathcal{U}_R$ be the homogeneous region outside of Ω_R; that is, $\mathcal{U}_R = \{(r,\theta) : r > R, 0 < \theta < \pi\}$. Refer to Fig. 1 for the complete problem geometry.

Submitted On: June 19, 2011
Accepted On: August 9, 2011

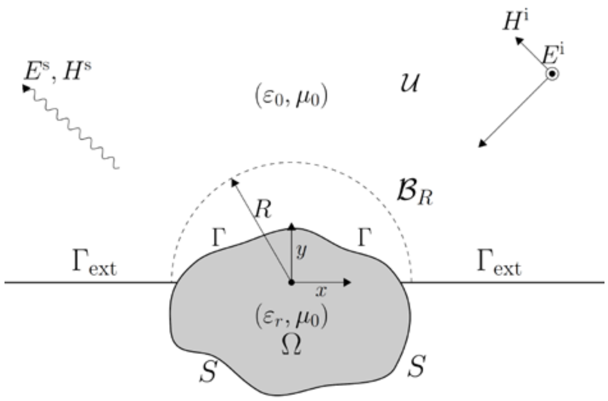

Fig. 1. Problem geometry – TM polarization depicted.

The following formulation is modeled after Van and Wood [13]. In this case, the magnetic field H is transverse to the z-axis so that E and H are of the form $E = (0,0,E_z)$ and $H = (H_x, H_y, 0)$. In this case, the nonzero component of the total electric field E_z satisfies the following boundary value problem:

$$\begin{aligned} -\Delta E_z + \varepsilon_r \frac{\partial^2 E_z}{\partial t^2} = 0 \quad & \text{in } \Omega \cup \mathcal{U} \times (0,\infty), \\ \frac{\partial E_z}{\partial t} = -\frac{\eta}{\mu}\frac{\partial E_z}{\partial \mathbf{n}} \quad & \text{on } S \cup \Gamma_{\text{ext}} \times (0,\infty), \quad (1) \\ E_z|_{t=0} = E_0, \quad & \\ \frac{\partial E_z}{\partial t}\Big|_{t=0} = E_{t,0} \quad & \text{in } \Omega \cup \mathcal{U} \end{aligned}$$

where $\varepsilon_r = \varepsilon / \varepsilon_0$ is the relative electric permittivity, E_0 and $E_{t,0}$ are the given initial conditions and $\eta = \sqrt{\mu_r / \varepsilon_r}$ is the normalized intrinsic impedance of the infinite ground plane. We are assuming that we have a non-dispersive material in the cavity, or that the permittivity is not a function of frequency, but could vary with respect to position. That is, we are assuming that the impedance is constant in the time domain. We observe the scattered field E_z^s solves:

$$\begin{aligned} -\Delta E_z^s + \frac{\partial^2 E_z^s}{\partial t^2} &= 0 \quad \text{in } \mathcal{U} \times (0,\infty), \\ \frac{\partial E_z^s}{\partial t} + \frac{\eta}{\mu}\frac{\partial E_z^s}{\partial \mathbf{n}} &= -\left(\frac{\partial E_z^i}{\partial t} + \frac{\eta}{\mu}\frac{\partial E_z^i}{\partial \mathbf{n}}\right), \quad (2) \\ & \text{on } \Gamma_{\text{ext}} \cup \Gamma \times (0,\infty), \end{aligned}$$

and also satisfies the appropriate radiation condition at infinity.

The homogeneous region $\mathcal{U}$ above the protruding cavity is assumed to be air and hence, its permittivity is $\varepsilon_r = 1$. In $\mathcal{U}$, the total field can be decomposed as $E_z = E_z^i + E_z^s$ where E_z^i is the incident field, and E_z^s the scattered field.

III. SEMIDISCRETE PROBLEM

We will first decompose the entire solution domain to two sub-domains via an artificial semicircle, $\mathcal{B}_R$, which entirely encloses the overfilled cavity (refer to Fig. 2). These two sub-domains consist of the infinite upper half plane over the impedance plane exterior to the semicircle, denoted $\mathcal{U}_R$, and the cavity plus the interior region of the semicircle, denoted Ω_R.

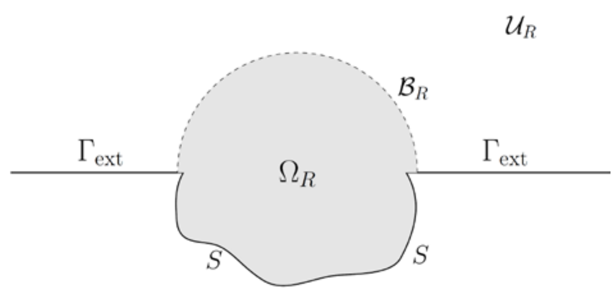

Fig. 2. Sub-domains.

For this problem, as in [13], we will choose to use the Newmark scheme, an implicit time-stepping method that offers the advantage of stability. It is defined by the following: let N be a positive integer, T be the time interval, $\delta t = T / N$ be the temporal step size, and $t_{n+1} = (n+1)\delta t$ for $n = 0,1,2,\ldots,N-1$. The following are approximations at $t = t_{n+1}$:

$$u^{n+1} \approx u, \qquad \dot{u}^{n+1} \approx \frac{\partial u}{\partial t}, \qquad \ddot{u}^{n+1} \approx \frac{\partial^2 u}{\partial t^2}.$$

We further define γ and β as parameters to be determined to guarantee stability of the scheme, $\alpha^2 = \dfrac{1}{(\delta t)^2 \beta}$, and $\tilde{u}$ denotes predicted values.

Therefore, it can be shown that the scattered field $u^{s,n+1}$ satisfies the following *exterior problem*:

$$\begin{aligned} &-\Delta u^{s,n+1} + \alpha^2 u^{s,n+1} = \alpha^2 \tilde{u}^{s,n+1} \quad \text{in } \mathcal{U}_R, \\ &u^{s,n+1}(R,\theta) = g(R,\theta) \quad \text{on } \mathcal{B}_R, \\ &\delta t \gamma \alpha^2 u^{s,n+1} + \frac{\eta}{\mu}\frac{\partial u^{s,n+1}}{\partial n} = \\ &\qquad \delta t \gamma \alpha^2 \tilde{u}^{s,n+1} - \tilde{\tilde{u}}^{s,n+1} \ \text{on}\, \Gamma_{\text{ext}}, \end{aligned} \tag{3}$$

where $g \overset{def}{=} u^{n+1} - u^{i,n+1}$ and the radiation condition is satisfied.

Therefore, we seek the solution for the nonhomogeneous modified Helmholtz equation $-\Delta u(\mathbf{r}) + \alpha^2 u(\mathbf{r})) = f((\mathbf{r}))$, where $\mathbf{r}$ denotes location and $f(\mathbf{r}) = \alpha^2 \tilde{u}^{s,n+1}(\mathbf{r})$. This equation is subject to nonhomogeneous boundary conditions of the form $Au(\mathbf{r}_s) + B\dfrac{\partial u(\mathbf{r}_s)}{\partial \mathbf{n}} = h(\mathbf{r}_s)$, where $\mathbf{r}_s$ is on the surface and $\mathbf{n}$ is the outward unit normal, A and B are constants defined as $A = \Delta t \gamma \alpha^2$ and $B = \dfrac{\eta}{\mu}$, and $h(\mathbf{r}_s) = \Delta t \gamma \alpha^2 \tilde{u}^{s,n+1} - \tilde{\tilde{u}}^{s,n+1}$.

IV. INTEGRAL REPRESENTATION OF SOLUTION AND GREEN'S FUNCTION

The integral representation of the solution in the exterior domain (the annular sector depicted in Fig. 3) can be shown to be, for $\mathrm{r} \in \mathcal{U}_R$ and source location at r':

$$\begin{aligned} u(r) = &\iint_{\mathcal{U}_R} f(r') G(r \mid r') dS' - \\ &\frac{1}{A}\int_{\Gamma_{\text{ext}}} h(r') \frac{\partial G(r \mid r')}{\partial n'} dr' + \\ &\int_{\mathcal{B}_R} \left(G(r \mid r') \frac{\partial u(r')}{\partial n'} - u(r') \frac{\partial G(r \mid r')}{\partial n'} \right) d\theta'. \end{aligned} \tag{4}$$

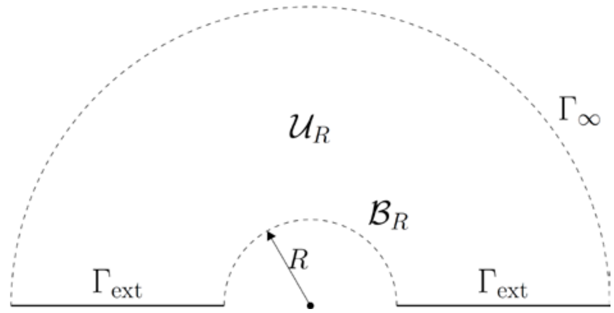

Fig. 3. Exterior domain.

The Green's function has been developed from several sources for an impedance half-plane, see for example, [15-17]. We follow Durán, *et al.*, in [11] to obtain the following, noting the integral expression may be simplified through residue analysis:

$$\begin{aligned} G(r \mid r') = &\frac{1}{2\pi} K_0(\alpha R) - \frac{1}{2\pi} K_0(\alpha R^*) \\ &- \frac{2B}{4\pi} \int_{-\infty}^{\infty} \frac{e^{-\sqrt{\xi^2+\alpha^2}\,(y'+y)}}{(A - B\sqrt{\xi^2+\alpha^2})} e^{i(x'-x)\xi} d\xi. \end{aligned} \tag{5}$$

We note $R = \sqrt{(x'-x)^2 + (y'-y)^2}$ and $R^* = \sqrt{(x'-x)^2 + (y'+y)^2}$. At this point, we implement an integral equation method along the artificial boundary, $\mathcal{B}_R$, to couple the solution along the artificial boundary through the Dirichlet-to-Neumann mapping, or Steklov-Poincaré operator. Following Hsiao, *et al.*, in [18], where we define $\varphi(r') = \dfrac{\partial u(r')}{\partial n_{r'}}$, all of the boundary integral operators for $r \in \mathcal{B}_R$ are expressed as follows:

$$(S\varphi)(r) = \int_{\mathcal{B}_R} G(r \mid r') \varphi(r') d\theta',$$

$$(Du)(r) = \int_{\mathcal{B}_R} u(r') \frac{\partial G(r \mid r')}{\partial n'} d\theta',$$

$$(A\varphi)(r) = \int_{\mathcal{B}_R} \frac{\partial G(r \mid r')}{\partial n} \varphi(r') d\theta',$$

$$(Hu)(r) = -\int_{\mathcal{B}_R} u(r') \frac{\partial}{\partial n} \frac{\partial G(r \mid r')}{\partial n'} d\theta.$$

We further define the Newton Potential to consist of the following terms, for $r \in \mathcal{B}_R$:

$$(Nf)(r) = \iint_{\mathcal{U}_R} f(r')G(r \mid r')dS',$$

$$(Ph)(r) = -\frac{1}{A}\int_{\Gamma_{\text{ext}}} h(r')\frac{\partial G(r \mid r')}{\partial n'}dx'.$$

The mapping properties are well-established for the preceding boundary integral operators. As a result, as in [18] or [19], we define $\mathcal{T}_R : H^{1/2}(\mathcal{B}_R) \to H^{-1/2}(\mathcal{B}_R)$ as a bounded Steklov-Poincaré operator as follows:

$$(\mathcal{T}_R u)(r) = S^{-1}(\frac{1}{2}I + D)u(r)$$
$$= \left[(\frac{1}{2}I + A)S^{-1}(\frac{1}{2}I + D) + H\right]u(r).$$

The second expression is the symmetric expression of the operator. In addition, the following theorem, similar to Cakoni and Colton's Theorem 5.20 in [20], also applies:

Theorem 1 *The Steklov-Poincaré operator,* $\mathcal{T}_R$ *, is a bounded, linear operator from* $H^{1/2}(\mathcal{B}_R) \to H^{-1/2}(\mathcal{B}_R)$*. Also, the principal part of* $\mathcal{T}_R$ *, referred to as* $\mathcal{T}_{R,P}$ *, satisfies the coercivity estimate:*

$$-\langle \mathcal{T}_{R,P}u, u\rangle \geq C\ \|u\|^2_{H^{1/2}(\mathcal{B}_R)}$$

for some $C > 0$*, such that the difference* $\mathcal{T}_R - \mathcal{T}_{R,P}$ *is a compact operator from* $H^{1/2}(\mathcal{B}_R) \to H^{-1/2}(\mathcal{B}_R)$.

V. VARIATIONAL FORMULATION

Instead of enforcing the boundary conditions on the test function space V as in [1], we choose to define the subspace V simply as $H^1(\Omega_R)$. The variational formulation will then be to find $u \in V$ such that:

$$b_{TM}(u,v) = F(v) \qquad \forall v \in V. \tag{6}$$

We define the sesquilinear term:

$$\begin{aligned} b_{TM}(u,v) = &\int_{\Omega_R} \nabla u \cdot \nabla \overline{v} dxdy - \int_{\mathcal{B}_R} \mathcal{T}_R u\overline{v} d\ell \\ &+ \frac{\mu}{\eta}\Delta t\gamma\alpha^2 \int_S u\overline{v}d\ell \\ &+ \alpha^2 \int_{\Omega_R} \varepsilon_r u\overline{v}dxdy, \end{aligned} \tag{7}$$

as well as the bounded conjugate linear functional term:

$$\begin{aligned} F(v) = &\int_{\mathcal{B}_R} J\overline{v}d\ell - \int_{\mathcal{B}_R} \Psi\tilde{u}^s\overline{v}d\ell \\ &+ \frac{\mu}{\eta}\Delta t\gamma\alpha^2 \int_S \tilde{u}\overline{v}d\ell \\ &- \frac{\mu}{\eta}\int_S \tilde{\tilde{u}}\overline{v}d\ell + \alpha^2 \int_{\Omega_R} \varepsilon_r \tilde{u}\overline{v}dxdy, \end{aligned} \tag{8}$$

and we further define the bounded terms:

$$(\Psi_R \tilde{u}^{s,n+1})(r) = S^{-1}((N\tilde{u}^{s,n+1})(r) + (P\tilde{u}^{s,n+1})(r))$$

and $\qquad J = \dfrac{\partial u^i}{\partial r}\Big|_{r=R} - \mathcal{T}_R u^i.$

Theorem 2 *The variational problem (6) is well-posed: a solution* $u \in V$ *exists, is unique, and for* $C > 0$*:*

$$\|u\| \leq C\left[\|u^i\| + \|\tilde{u}^s\| + \|\tilde{u}\| + \|\tilde{\tilde{u}}\| + \|\varepsilon_r \tilde{u}\|\right].$$

Using the results of the previous section, and writing $b_{TM}(u,v)$ as the sum of a coercive operator and compact operator, (6) can be shown to be well-posed through variational methods.

VI. NUMERICAL RESULTS

A. Planar cavity results

We ran a numerical study on a planar cavity to provide a context for the theory. We ran the data for two separate cases: a perfect electrical conducting (PEC) surface on the plane Γ_{ext} and PEC surface on the cavity walls, S, and a PEC plane and impedance boundary conditions (IBC) on the cavity walls. The idea is to see the progression as we introduce IBC on a strict PEC surface, in which we would expect more attenuation as the surface changes.

The numerical model was set up as depicted in Fig. 4, using an incident Gaussian Pulse with $\delta t = 0.0625$, $\varepsilon_r = 2$, $\mu_0 = 1$, and Newmark parameters $\gamma = 0.95$ and $\beta = 0.5256$ to ensure stability. The visual depictions of the electric field are plotted against time as measured in light meters (LM), which is the amount of time light travels in one meter of free space.

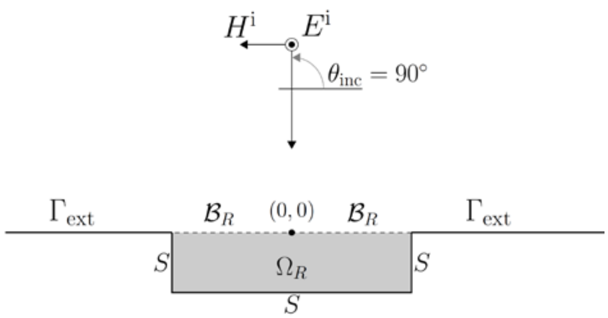

Fig. 4. Shallow cavity (1m by 0.25m).

The first run is depicted in Fig. 5. With the PEC plane and PEC cavity walls as a benchmark, we observe that the case with IBC enforced at the cavity walls ($\eta = 0.8$) exhibits more attenuated characteristics. We also observe the stability of the Newmark scheme over time.

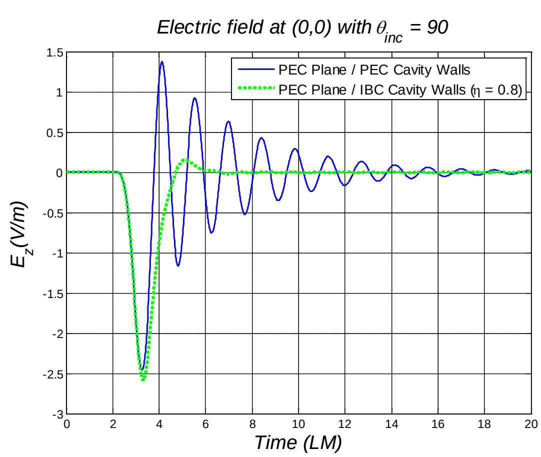

Fig. 5. Shallow cavity with $\eta = 0.8$.

We also want to observe the effects as $\eta \to 0$, as we would expect the field to exhibit the characteristics of a strict PEC on the plane and cavity walls. This is clearly evident in Fig. 6 with the PEC plane and IBC cavity walls simulation showing more oscillatory behavior as in the strict PEC case. Again, we observe the stability of the Newmark scheme over time.

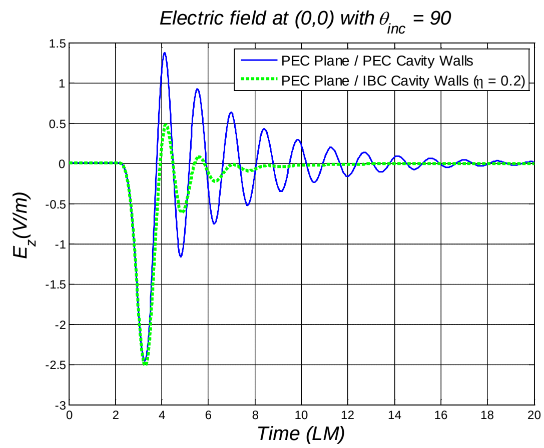

Fig. 6. Shallow cavity with $\eta = 0.2$.

We also wanted to observe the effects of changing boundary conditions on the radar cross section of the cavity model. We ran two simulations, at the selected frequencies of 289.5 MHz and 480.45 MHz, as depicted in Fig. 7 and Fig. 8.

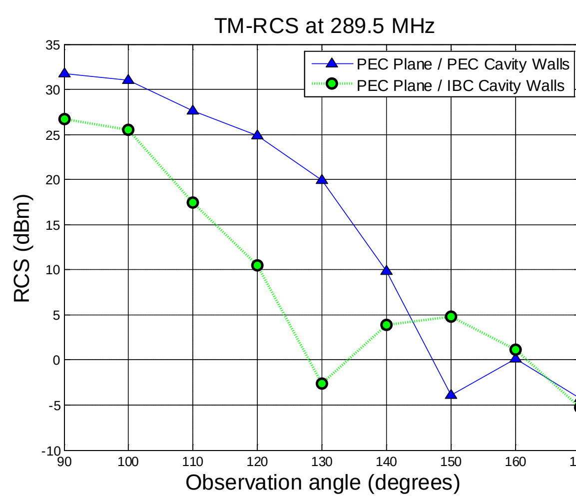

Fig. 7. Shallow cavity RCS at 289.5 MHz.

In both cases, we observe the expected lobing, and note the fact that as the frequency is increased to 480.45 MHz, the separation in RCS values between the two cases is more apparent. More specifically, for 480.45 MHz, the RCS values are lower as the boundary conditions approach a complete IBC on the cavity walls.

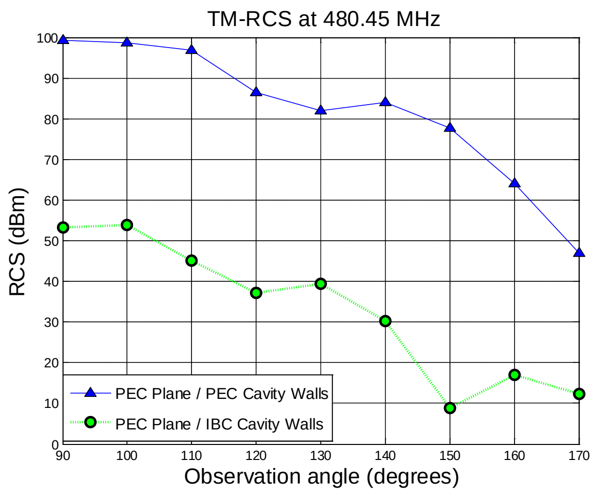

Fig. 8. Shallow cavity RCS at 480.45 MHz.

B. Overfilled cavity results

As with the planar cavity, we used the same set of parameters for the overfilled cavity depicted in Fig. 9.

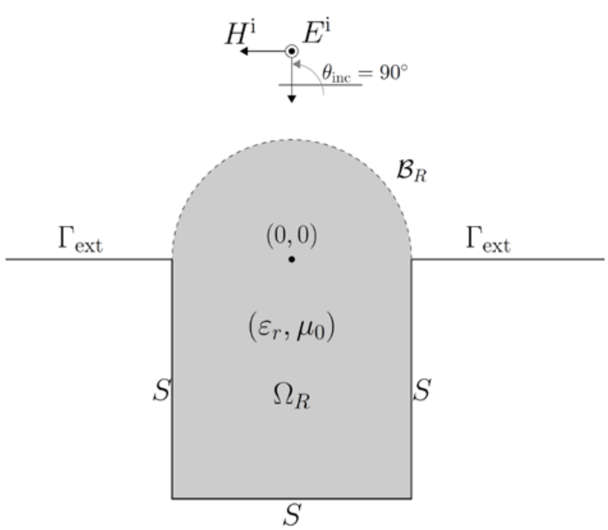

Fig. 9. Overfilled cavity (1m deep; 0.5m radius).

However, in this model, we add a third case of an IBC on both the cavity walls and plane. We also chose an observation point at the origin. We note in both Fig. 10 and Fig. 11 that the depicted scattered field becomes more attenuated as the boundary conditions for the plane and cavity walls approach an IBC surface. The observation is truncated at 50 LM for scaling, but the simulations exhibit the same stability as with the planar case beyond this point. It is also evident that the fields are more oscillatory than the shallow cavity due to the presence of more material both above and below the observation point. We also note in Fig. 11 that as $\eta \to 0$ the field begins to exhibit the characteristics of a strict PEC surface, as seen in the more oscillatory behavior of the IBC plane and IBC cavity walls condition.

We also present the RCS data in Fig. 12 for 289.5 MHz and Fig. 13 for 480.45 MHz. Again, we notice similar behavior at the lower frequency for all three cases; however, at a higher frequency, we observe both the expected lobing and the more attenuated results as the IBC is enforced on both the cavity walls and the plane.

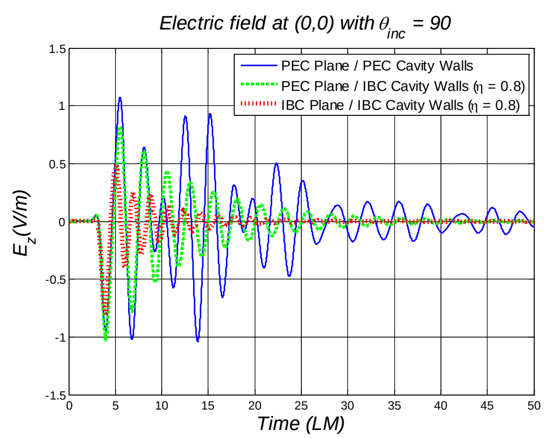

Fig. 10. Overfilled cavity with $\eta = 0.8$.

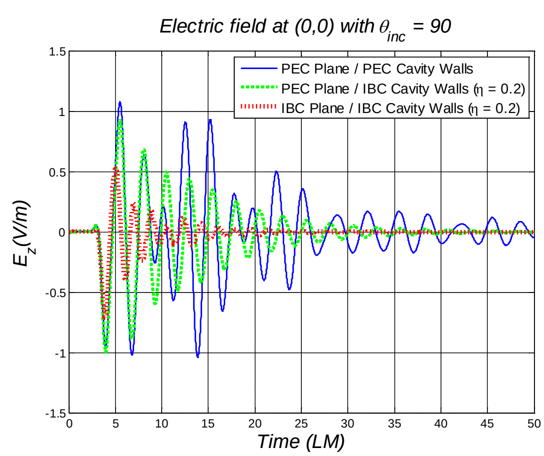

Fig. 11. Overfilled cavity with $\eta = 0.2$.

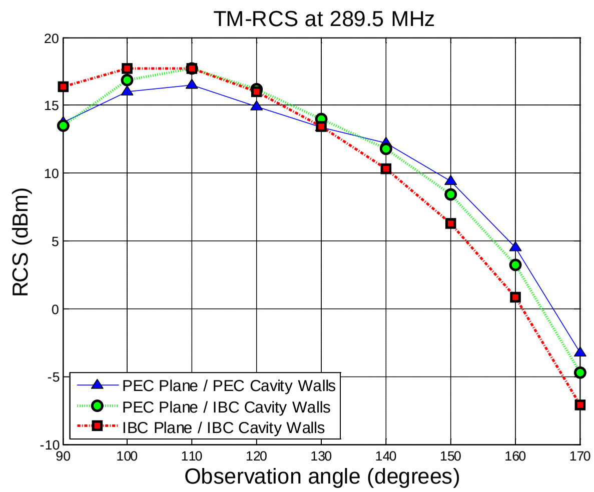

Fig. 12. Overfilled cavity RCS at 289.5 MHz.

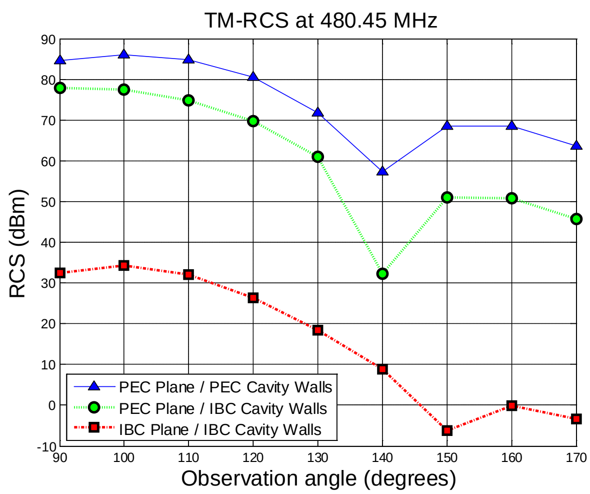

Fig. 13. Overfilled cavity RCS at 480.45 MHz.

VII. CONCLUSION

We present a mathematical model for analyzing transient electromagnetic scattering induced by an overfilled cavity embedded in an impedance ground plane. We have established the well-posedness of the problem through a variational formulation, and this sets the foundation for numerical implementation through a hybrid finite element - boundary integral technique. We present electric field and RCS data for both a simplified planar cavity as well as the overfilled cavity model, which both exhibit expected results.

ACKNOWLEDGMENT

The views expressed in this article are those of the authors and do not reflect the official policy or position of the United States Air Force, Department of Defense, or the U. S. Government.

REFERENCES

[1] J. M. Jin, S. Ni, and S. W. Lee, "Hybridization of SBR and FEM for Scattering by Large Bodies with Cracks and Cavities," *IEEE Trans. Antennas Propag.*, vol. 43, no. 10, pp. 1130-1139, 1995.

[2] L. C. Kempel and J. L. Volakis, "Scattering by Cavity-Backed Antennas on a Circular Cylinder," *IEEE Trans. Antennas Propag.,* vol. 42, no. 10, pp. 1268-1279, 1994.

[3] J. Liu and J. M. Jin, "A Special Higher Order Finite-Element Method for Scattering by Deep Cavities," *IEEE Trans. Antennas Propag.,* vol. 48, no. 5, pp. 694-703, 2000.

[4] W. D. Wood and A. W. Wood, "Development and Numerical Solution of Integral Equations for Electromagnetic Scattering from a Trough in a Ground Plane," *IEEE Trans. Antennas Propag.,* vol. 47, no. 8, pp. 1318-1322, 1999.

[5] C. J. Reddy, M. D. Deshpande, B. R. Cockrell, and F. B. Beck, "Fast Frequency Response Calculations of Cavity-Backed Aperture Antennas using Hybrid FEM/MoM Technique in Conjunction with Model Based Parameter Estimation," *Applied Computational Electromagnetic Society (ACES) Journal*, vol. 13, no. 3, pp. 283-290, 1998.

[6] D. Caratelli and A. Yarovoy, "Design and Full-Wave Analysis of Cavity-Backed Resistively Loaded Circular-End Bow-Tie Antennas for GPR Applications – Part I," *Applied Computational Electromagnetic Society (ACES) Journal*, vol. 25, no. 10, pp. 809-817, 2010.

[7] H. Ammari, G. Bao, and A. Wood, "A Cavity Problem for Maxwell's Equations," *Meth. Math. Appl.*, vol. 9, no. 2, pp. 249-260, 2002.

[8] T. Van and A. Wood, "Analysis of Time-Domain Maxwell's Equations for 3-D Cavities," *Adv. Comput. Math.*, vol. 16, nos. 2-3, pp. 211-228, 2002.

[9] T. Van and A. Wood, "A Time-Marching Finite Element Method for an Electromagnetic Scattering Problem," *Math. Meth. Appl. Sci.*, vol. 26, no. 12, pp. 1025-1045, 2003.

[10] T. Van and A. Wood, "A Time-Domain Finite Element Method for Maxwell's Equations," *SIAM J. Numer. Anal.*, vol. 42, no. 4, pp. 1592-1609, 2004.

[11] M. Durán, I. Muga, and J.-C. Nédélec, "The Helmholtz Equation in a Locally Perturbed Half-Plane with Passive Boundary," *IMA J. Appl. Math.*, vol. 71, no. 6, pp. 853-876, 2006.

[12] A. W. Wood, "Analysis of Electromagnetic Scattering from an Overfilled Cavity in the Ground Plane," *J. Comput. Phys.*, vol. 215, no. 2, pp. 630-641, 2006.

[13] T. Van and A. W. Wood, "Analysis of Transient Electromagnetic Scattering from Overfilled Cavities," *SIAM J. Appl. Math.*, vol. 64, no. 2, pp. 688-708, 2004.

[14] J. Huang, A. W. Wood, and M. J. Havrilla, "A Hybrid Finite Element-Laplace Transform Method for the Analysis of Transient Electromagnetic Scattering by an Over-Filled Cavity in the Ground Plane," *Commun. Comput. Phys.*, vol. 5, no. 1, pp. 126-141, 2009.

[15] M. Durán, I. Muga, and J.-C. Nédélec, "The Helmholtz Equation in a Locally Perturbed Half-Space with Non-Absorbing Boundary," *Arch. Ration. Mech. An.*, vol. 191, no. 1, pp. 143-172, 2009.

[16] R. O. Hein-Hoernig, *Green's Functions and Integral Equations for the Laplace and Helmholtz Operators in Impedance Half-Spaces*, Ph.D. Thesis, École Polytechnique, 2010.

[17] C. G. Politis, M. V. Papalexandris, and G. A. Athanassoulis, "A Boundary Integral Equation Method for Oblique Water-Wave Scattering by Cylinders Governed by the Modified Helmholtz Equation," *Appl. Ocean Res.*, vol. 24, no. 4, pp. 215-233, 2002.

[18] G. C. Hsiao, O. Steinbach, and W. L. Wendland, "Domain Decomposition Methods via Boundary Integral Equations," *J. Comput. Appl. Math.*, vol. 125, no. 1, pp. 521-537, 2000.

[19] O. Steinbach and W. L. Wendland, "On C. Neumann's Method for Second-Order Elliptic Systems in Domains with Non-Smooth Boundaries," *J. Math. Anal. Appl.*, vol. 262, no. 2, pp. 733-748, 2001.

[20] F. Cakoni and D. Colton, *Qualitative Methods in Inverse Scattering Theory*, Springer-Verlag, Berlin, Germany, 2006.

Robert S. Callihan received his B.S. from the U. S. Air Force Academy in mathematics, and his M.B.A. from Georgia College and State University. He currently is a Ph.D. candidate at the Air Force Institute of Technology. He has served 18 years in the Air Force, primarily as a trainer pilot and KC-135 tanker pilot. He most recently served on the faculty as an Assistant Professor of Mathematical Sciences at the U. S. Air Force Academy, and will return to that assignment following his dissertation. Lieutenant Colonel Callihan's research interests are partial differential equations and Green's functions.

Aihua W. Wood received her B.S. from Beijing University and Ph.D. from the University of Connecticut in Mathematics. She served as an Assistant Professor at the Naval Postgraduate School for three years and the Pennsylvania State University at Erie for one year before joining the faculty at the Air Force Institute of Technology in 1994. She has been a Professor of Mathematics since 2002 and is currently the institute's Equity Advisor. Dr. Wood's research interests include partial differential equations, electromagnetic wave propagation, and rarefied gas dynamics.